04

Synthesis of boron carbide by the electric arc method in open air from carbon of various origins

© R.S. Martynov,[1] A.Ya. Pak,[1] G.Ya. Mamontov,[1] O.G. Volokitin,[2] S.A. Yankovsky,[1,3] A.A. Gumovskaya,[1] P.V. Povalyaev,[1,3] Zh. Bolatova[1]

[1] Tomsk Polytechnic University, Tomsk, Russia
[2] Tomsk state university of architecture and building, Tomsk, Russia
[3] Federal State Budgetary Educational Institution of Higher Education, Kemerovo,. Russia
e-mail: rsm6@tpu.ru

Received July 12, 2022
Revised October 25, 2022
Accepted October 27, 2022

The paper presents the results of experimental studies on the implementation of electric arc synthesis of boron carbide using carbon with different morphology and origin as a feedstock: carbon fibers, flake graphite, carbon obtained by pyrolysis of plant waste, namely, pine sawdust and cedar nuts husks. A feature of the electric arc method used is its implementation using an original plasma reactor using atmospheric air as a working gas medium. Oxidation of feedstock and synthesis products in the working cycle of the reactor is prevented due to the generation of CO and CO_2 gases in the reaction zone. The possibility of obtaining a material containing micron and submicron boron carbide crystals in a graphite matrix has been experimentally shown. Also, the paper presents information about the features of the oxidation processes of the obtained materials in comparison with commercial samples of boron carbide.

Keywords: boron carbide, electric arc synthesis, carbon fibers, flake graphite, carbon of plant origin.

DOI: 10.21883/TP.2023.01.55441.183-22

Introduction

The boron carbide is a known ultra-hard material to be applied in various field of science and technics [1]. The boron carbides are characterized by a wide area of homogeneity, high hardness (up to 35 GPa), a relatively low density 2.52 g/cm^3 [2]. The most widespread approach to synthesis of boron carbide is carbon-thermal and magnesium-thermal recovery using ovens of a various operation principle [1,3] as well as a baking method [4]. The less widespread, but still known are the approaches based on generation of ion [5] and electron [6] high-intense flows of energy, the plasma jets [7], production of high pressure [8]. Various composites are widely known and they are based on the boron carbide and some specific morphological types of carbon materials, like, for example, carbon fibers [9–11]. These materials can exhibit the anisotropy of the properties [12,13], which is largely specified by the carbon matrix, on which crystals of boron carbide are formed. In recent years, attention has been largely directed to using the renewables as carbon obtained as a result of processing of plant biomass [14,15]. Various wood species and wood-processing waste are often used as a carbon source for synthesis of the so-called biomorphic carbides [16,17]. The largest scope of publications in the field of synthesis and investigation of the properties of the biomorphic carbides is dedicated to silicon carbide (90% of the total scope of the publications), 5% of the works is dedicated to titanium carbide, 3% of the works is dedicated to the zirconium carbide, while the other carbides occupy only 2% [18]. On the one hand, using plant precursors or carbon from waste allows providing the synthesis processes with renewable feedstock (which is especially important in the concept of the carbon footprint reduction [19]), and on the other hand, in some cases it makes it possible to achieve the special morphology and specific properties of the obtained carbide or composite based thereon [20]. It is obvious that a large variety of the natural forms and all possible waste, which can be used as carbon sources, provides great opportunities for synthesis of specially-morphologic materials. Thus, the present work is aimed at obtaining boron carbide-based materials using carbon feedstock of the various origins and morphology.

1. Materials and methods

The initial feedstock included two commercial kinds of carbon — flake oriented graphite (Heepani Tools Store, China) and carbon micro-sized fibers (Heepani Tools Store, China), as well as two kinds of plant carbon obtained from pine sawdust and cedar nuts husks by pyrolysis.

Each kind of the initial biomass was preliminarily ground to specific dimensions (the sieve residue 200−500 μm). The prepared analytical samples of sawdust and cedar nuts husks were separately weighed on the analytical scales VIBRA HT-224RCE, whereas each weighed amount of biomass was

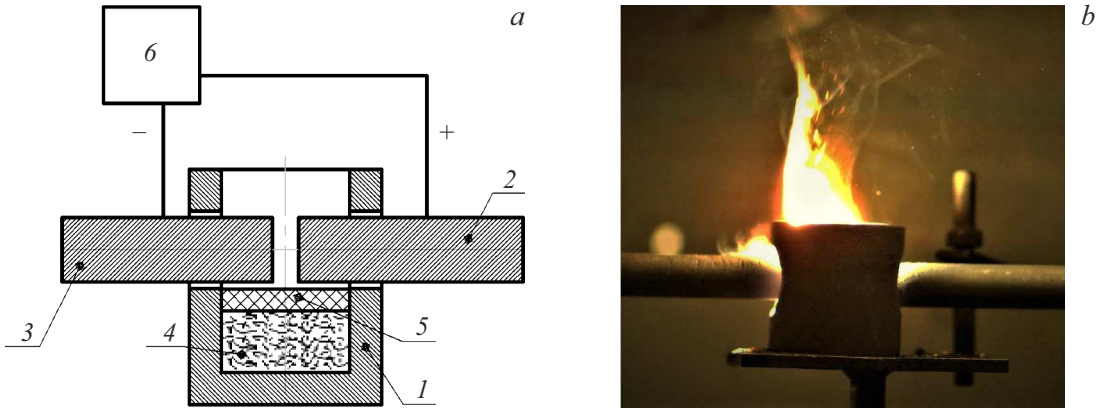

Figure 1. *a* — the reactor diagram in section: *1* — the crucible, *2* — the anode, *3* — the cathode, *4* — the mixture of the initial reagents, *5* — the felt gasket, *6* — the direct current source; *b* — the photogram of the synthesis process.

200 g. The pine sawdust were placed in a heat-resistance galvanized container to fully fill its space and tightly covered with a cap. The identical container comprised the weighed amount of cedar nuts husks. The two prepared containers were place in a thermally-controlled oven PM-1400 with the temperature control accuracy of $\pm 1^\circ$C. The temperature in the oven was heated at the rate 20°C/min to achieve the specified value (600°C). The holding time was one clock hour, then the temperature maintenance was switched off and the thermally-controlled oven was naturally cooled to the room temperature. The obtained biocarbon was extracted out of each container and weighed. Then, the weighed amounts of the obtained biocarbon were prepackaged and transferred for further studies.

Each type of carbon was mixed with the powder of amorphous boron (Heepani Tools Store, China) inside the ball mill Horiba Sample SpexPrep during 30 min. Two types of the mixtures were prepared: 1) — the stoichiometric mixture of boron and ultrafine carbon of the „Sibunit“ — grade for the first series of the experiments in order to optimize the modes of the arc reactor; 2) — with twofold excess of carbon in order to ensure preservation of features of the morphology of the initial feedstock after the synthesis process.

The obtained mixtures were loaded into a graphite crucible, with subsequently pushing therein a horizontally graphite cylindrical anode and cathode manufactured as rods of the diameter of 8 mm. The initial reagents were additionally covered with a felt gasket and then heated by direct current arc discharge plasma in a plasma reactor [21,22] at the source's pre-set amperage of 200 A and with the heating duration of up to 45 s. The intensity of thermal impact was controlled by varying the distance from the arch discharge (the longitudinal axis of the anode and cathode) to a graphite crucible's bottom holding the initial mixtures. The specific design features of the reactor and its operation modes had been selected based on the previous works for obtaining boron carbide in the electric arc method [23]. After the plasma impact and cool-down of the elements of the arc reactor the obtained materials were extracted out of the graphite crucibles and analyzed.

The X-ray diffraction analysis was carried out at the Shimadzu XRD 7000s diffractometer (CuK_α-radiation). The scanning electron microscopy was carried out on the TESCAN VEGA 3 SBU microscope (TGU) with the energy-dispersion analysis unit and on the Hitachi TM3000 microscope. The transmission electron microscopy was carried out on the JEOL JEM 2100F microscope (the samples were prepared by preparing an alcohol suspension in the ultra-sound bath).

The thermal decomposition of the obtained boron carbide samples was studied using the STA 449 F3 Jupiter differential thermal analyzer (Netzsch, Germany). It was analyzed at the heating rate 10°C/min in the corundum crucible with a perforated cap to the temperature 1000°C in order to fully oxidize it. The sample of the weight of about 20 mg was spread uniformly over the crucible bottom and place in a stream of an oxidizing medium (air). The gas flowrate was 150 ml/min. All the studies were under atmospheric pressure. The parameters of the process of thermal conversion of the boron carbide samples were comparatively evaluated based on the physical values (temperature, time and rate of the process), which were graphically calculated using thermogravimetric (TG), differential thermogravimetric (DTG) and differential scanning calorimetric (DSC) curves [24].

2. Results and discussion

During the process of the plasma processing of the initial mixtures of boron and carbon with the different morphology, the actually measured amperage was up to ~ 160 A at the arc stage with the electrode voltage ~ 40 V. The average power within the operating interval was at most ~ 6 kW, thereby ensuring the energy output up to ~ 230 kJ. The operation cycle's temperature of the external wall of the graphite crucible reaches $\sim 1800^\circ$C. Fig. 1 shows the

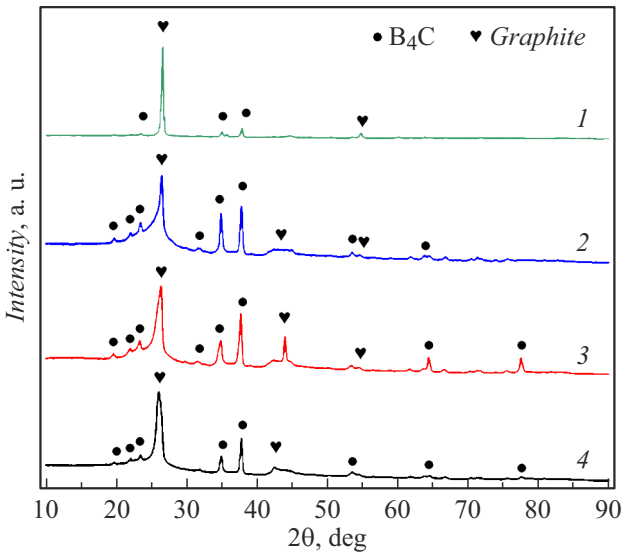

Figure 2. Typical picture of X-ray diffraction of the obtained materials using various kinds of the carbon materials: *1* — the flake graphite, *2* — the carbon fibers, *3* — the pyrolytic cedar nuts husks, *4* — the pyrolytic pine sawdust.

principal diagram of the plasma reactor and the photogram of the synthesis process.

Fig. 2 shows the X-ray diffraction patterns of the obtained four types of powders using the various carbon sources: flake graphite, carbon fibers, carbon, as obtained by the method of pyrolysis from the cedar nuts husks and from pine sawdust. All the X-ray diffraction pictures are characterized by two main crystal phases: graphite and boron carbide. Each X-ray diffraction picture identifies many diffraction maximums, in particular, in the areas $\sim 19.65°$, $\sim 22.02°$, $\sim 23.45°$, $\sim 31.83°$, $\sim 34.90°$, $\sim 37.69°$, which correspond to the crystal structure of boron carbide B4C. The graphite phase is distinctly identified by presence of the diffraction maximum at $\sim 26.6°$. A shape of this maximum and an intensity ratio of the main maximums of graphite and boron carbide differ on all the five typical pictures of X-ray diffraction. It can be primarily explained by the different nature of feedstock carbon, which is characterized by the various ratio of the crystal and amorphous components, morphological features and presence of the predominant orientation. It should be also noted that the designated phase of boron carbide is quite conditionally identified as $B_{12}C_3$ (B_4C) due to a known wide area of homogeneity of the boron carbides and almost unidentified differences between the reference and experimental pictures of the X-ray diffraction of the boron carbides with stoichiometry both as B_4C and $B_{13}C_2$ as well.

Fig. 3 shows the results of the scanning electron microscopy and the energy dispersion analysis of the chemical composition of the materials obtained. The synthesis products can be identified as having clusters of particles with sizes of about several hundred micrometers. Unambiguously, flat particles are identified in the samples obtained from oriented graphite and elongated cylindrical items are identified in the samples obtained from the carbon fibers. All the cases show a carbon matrix, whose surface has micro-sized particles of boron carbide formed. At the same time, no feature of the biomorphic structure is detected in the samples obtained using carbon of biological origin.

All the samples are identified with boron and carbon in approximately equal atomic portions and it is possible to identify presence of impurities (oxygen, silicon, aluminium, magnesium) of a slight content. The excessive carbon can be explained by the excess of this element in the composition of the initial feedstock (in comparison with the stoichiometric composition $B_{12}C_3$ (B_4C)), and by possible errors of the energy dispersion analysis, which are caused by non-uniformity of distribution of the particles in the synthesis products and presence of carbon in a substrate during the microscopy. Oxygen may be present due to possible surface oxidation of the particles. The magnesium traces can be present due to its availability in the initial feedstock, as this metal is used in boron manufacturing. The presence of silicon and aluminium in small portions can be explained by availability of oxides of silicon and aluminium almost everywhere, in particular, in the composition of the materials obtained from the biomass.

Fig. 4 shows the typical results of the transmission electron microscopy of the obtained samples. The composition of the synthesis product has had detected submicron particles with faceting features *1* of Fig. 4, *a*, which are characterized by the structure corresponding to the boron carbide (Table 1). The direct resolution mode makes it possible to view families of the planes with the interplanar distances ~ 4.52 and ~ 4.10 Å, which is also close to the structure of boron carbide. The particles are covered with a graphite shell with the interplanar distance of about ~ 3.50 Å. The synthesis products are also identified with items of sizes of several hundred nanometers with the graphite structure *2* of Fig. 4, *a*. When shifting an aperture diaphragm into an area of reflection corresponding to the sizes of the interplanar distances $\sim 3.40-3.60$ Å, the dark-field TEM images were obtained to highlight the shells of the particles (*1*, Fig. 4, *a*) and the items (*2*, Fig. 4, *a*). The data of the energy-dispersion analysis confirm the presence of carbon and boron in the clusters of the particles *1*, Fig. 4, *a*. As per the data of the energy-dispersion analysis, these clusters of the particles contain up to 75% wt. of boron, up to 9% wt. of carbon, up to 6% wt. of oxygen, up to 4% wt. of magnesium, up to 5% wt. of copper and up to 1% of the other chemical elements. The presence of boron and carbon should be considered as expected. The presence of magnesium is explained by initial boron available in its composition in the amount of several percent due to usage of this metal in production of boron from its oxide. The availability of oxygen is recorded almost in all the samples of any powders stored in air; in addition, as per mapping data of the chemical composition, oxygen is predominantly contained in the magnesium accumulation area; the oxygen

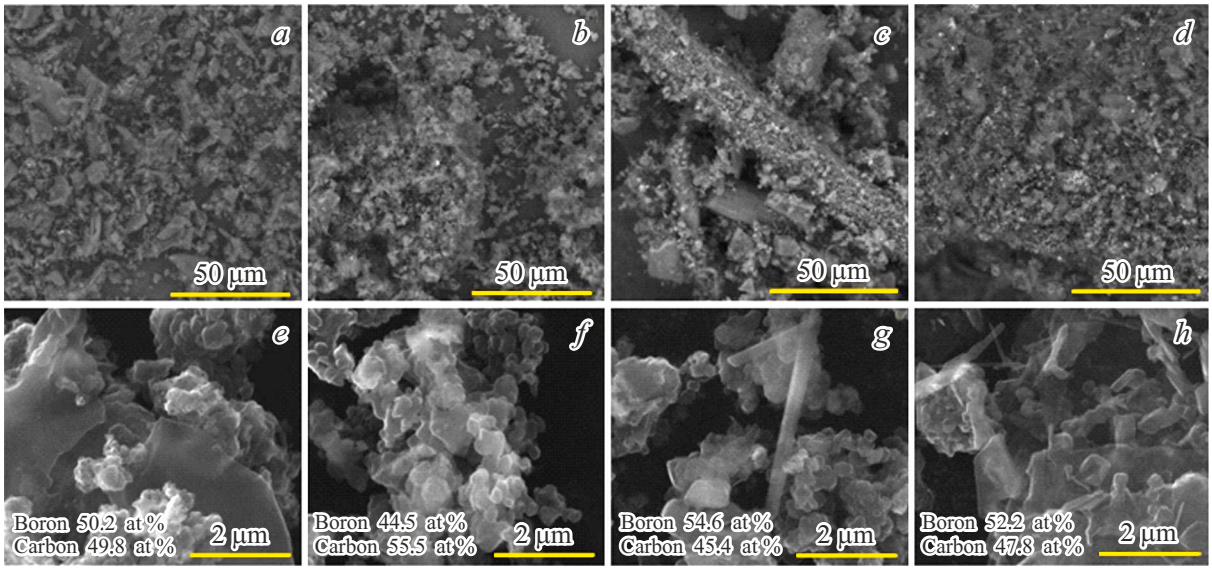

Figure 3. Results of the scanning electron microscopy and the energy dispersion analysis of the samples obtained using: *a, e* — carbon obtained from pine sawdust; *b, f* — carbon obtained from the cedar nuts husks; *c, g* — the carbon fibers; *d, h* — the oriented flake graphite.

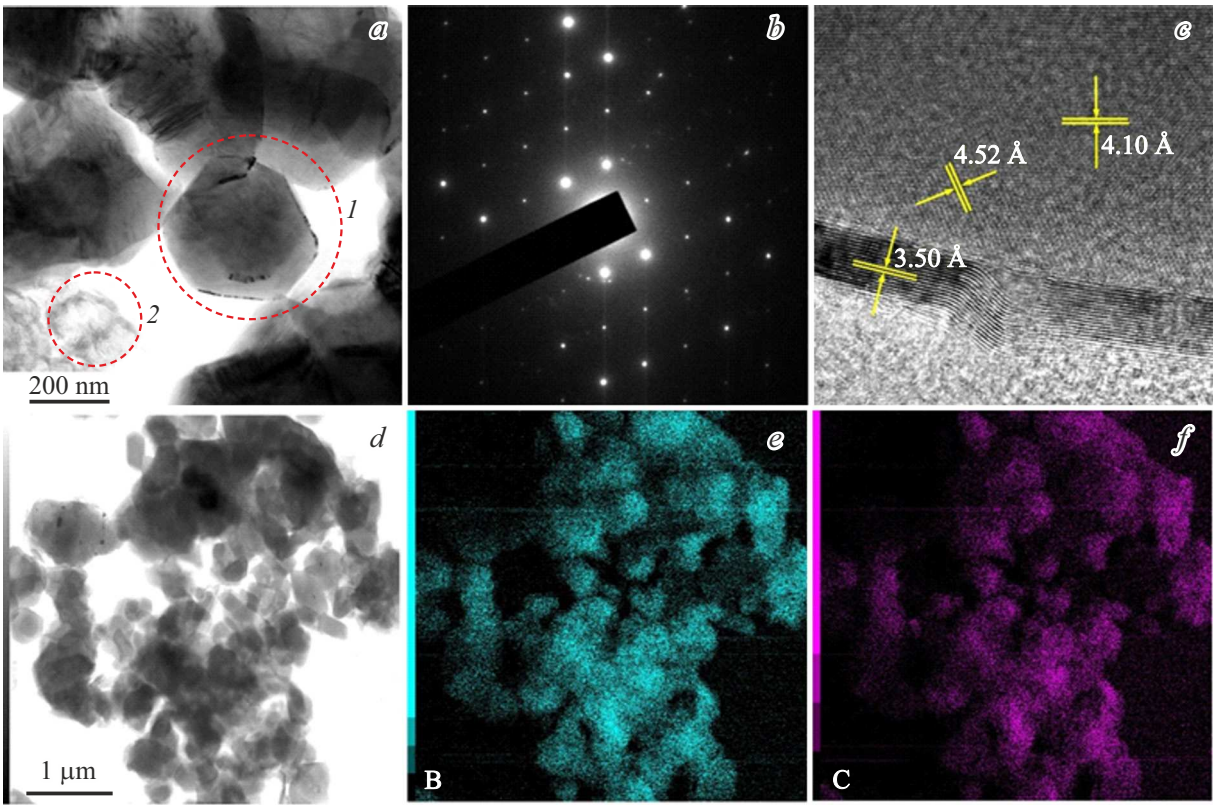

Figure 4. Typical results of the transmission electron microscopy: *a* — the light-field TEM-image; *b* — SAED from a separate crystal; *c* — the image in the direct resolution mode; *d* — the light-field STEM-image of the cluster for the energy-dispersion analysis; *e* — the boron distribution map; *f* — the map of carbon distribution in the cluster of the particles.

distribution map is not in contrast to the distribution map of boron and oxygen. The presence of copper in the samples is identified due to the fact that sample holders for the transmission electron microscope are made of copper.

The particles of boron carbide covered by the graphite shell can be formed due to known physical processes of crystallization of materials with a different melt temperature. Probably, during cooldown, the melt or vapor first of all

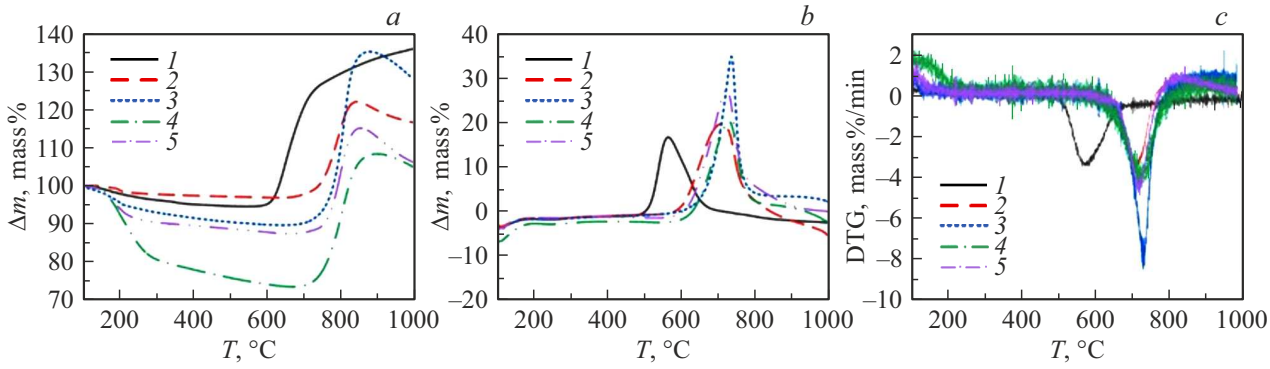

Figure 5. Data: *a* — TG, *b* — DSC, *c* — DTG of the oxidation process of the obtained samples of boron carbide BC_4 (medium−air (100 ml/min), the heating rate 10°C/min, the temperature interval from 100 to 1000°C); *1* — the commercial one, *2* — the cedar nuts husks, *3* — the carbon fibers, *4* — the flake graphite, *5* — the pine sawdust.

Table 1. Comparison of the standard and experimentally determined (by SAED data) interplanar distances *d*, Å

№	Fig. 4, *b*	Standard $B_{12}C_3$ (B_4C) № 35-798	Standard C № 1-640
1	4.47	4.52	–
2	3.98	4.05	–
3	3.46	–	3.39
4	2.58	2.58	–
5	2.40	2.39	–
6	1.88	1.90	–
7	1.74	1.76	–
8	1.61	1.62	1.69
9	1.46	1.47	–
10	1.32	1.32	1.32

forms the graphite shell, and there is a liquid material with boron and carbon therein, which forms a particle nucleus out of the boron carbide during crystallization. The presence of the particles with the „shell−nucleus“ structure is typical for the electric arc methods of obtaining the metals and non-metals, including the boron carbide, by using the direct current arc discharge plasma [25–27].

In order to understand the oxidation processes of the obtained samples of boron carbide synthesized based on the different kind of carbon, the differential thermal analysis is carried out in the oxidation medium. Fig. 5 shows the results of the experimental studies, the TG-, DSC- and DTG-curves of the boron carbide synthesized based on different kinds of carbon. The results of oxidation of the sample of commercial boron carbide are given as a standard example for comparison.

Boron carbide oxidizes in accordance with the known reaction, which is mentioned many times by the authors in the works [28–30]:

$$B_4C + 4O_2 = 2B_2O_3 + CO_2.$$

The start temperature of oxidation of commercial boron carbide starts at the temperature 600°C, which correlates to the data of the works [28–30].The start temperature of oxidation of the samples synthesized based on the different kinds of carbon in the present work is 709−726°C (Table 1), which is significantly higher in comparison with the start of the oxidation process of commercial boron carbide. The DTG data (Fig. 5, Table 2) make it possible to find that the maximum rate of oxidation of synthesized based on the different kinds of carbon was within the temperature interval 701−729°C and is characterized by a single-mode peak. In accordance with the above-given reaction, the full oxidation of boron carbide may cause the sample weight gain of up to 150%. The information about the change (increase) of the sample weight indicates incomplete oxidation of the samples of boron carbide (Table 2). The studied compositions have graphite (Fig. 2), which has a property of being thermally degraded at the temperatures above 900°C, thereby we observe a slight decrease of the weight within this temperature range. The results of the experimental studies make it possible to conclude that the synthesized samples, which are obtained with addition of carbon released from the different kind of biomass and graphite, have a higher oxidation resistance in comparison with commercial boron carbide. This phenomena may be related to the availability of the carbon matrix and the carbon shells designed to prevent the oxidation processes of the latter.

It should be noted that all the oxidation processes of boron oxide synthesized based on the different kinds of carbon proceed with substantial energy output in comparison with commercial boron carbide within the range of the higher temperatures.

Table 2. Results of the differential thermal analysis of the synthesized samples

Parameters/Carbon source	Boron carbide				
	Commercial	From cedar nuts husks	From carbon fibers	From flake graphite	From pine sawdust
Initial temperature of the intense oxidation, T_i, °C	600	715	721	709	726
Mass increment after oxidation, %	29	23	44	33	26
Final temperature of intense oxidation T_f, °C	725	835	855	871	845
Maximum rate of reaction $w_{\max}$, wt.% min	−3.38	−3.28	−7.35	−3.40	−4.47
Temperature of maximum rate of reaction $T_{\max}$, °C	566	705	729	701	711
Total time of active oxidation, τ_f, min	12.5	12	13.4	16.2	11.9

Conclusion

The work has presented the results of the experimental studies which demonstrate producibility of boron carbide using carbon of various origins as feedstock. In particular, it includes commercial carbon with special morphology, i.e. flake oriented graphite and micro-sized carbon fibers, as well as plant carbon obtained by pyrolysis of cedar nuts husks and pine sawdust.

The materials have been synthesized based on boron carbide, graphite and carbons formed by the classical pyrolysis out of commercial timber processing waste (pine sawdust) and food industry waste (cedar nuts husks), which in some cases inherit morphological features of the precursors. In doing so, no material was obtained so as to be classified as a biomorphic boron carbide. Nevertheless, the presented results make it possible to consider implementability of the boron carbide synthesis with involving the waste in the production cycle, i.e. carbon obtain by the biomass pyrolysis.

In accordance with the evaluations done, the energy capacity of this method's synthesis can be 64 (kW · h)/kg. However, the question of scaling of this process (including by changing the design of the non-vacuum plasma reactor) is still unresolved and requires further studies.

Thus, the implemented approach makes it possible to simultaneously reduce the energy capacity of the obtained material in comparison with its electric arc analogues by reducing power consumption for operation of the vacuum and gas distribution equipment.

Funding

The study has been carried out within the project FSWW-2022-0018 (State Assignment to Universities).

Conflict of interest

The authors declare that they have no conflict of interest.

References

[1] F. Thevenot. J. European Ceramic Societty, **6**, 205 (1990). DOI: 10.1016/0955-2219(90)90048-K
[2] M. Kakiage. J. POWTEC, **221**, 257 (2012). DOI: 10.1016/J.POWTEC.2012.01.010
[3] M.P.L.N. Rao, G.S. Gupta, P. Manjunath, S. Kumar, A.K. Suri, N. Krishnamurthy, C. Subramanian. J. IJRMHM, **27**, 621 (2009). DOI: 10.1016/J.IJRMHM.2008.10.004
[4] T.K. Roy, C. Subramanian, A.K. Suri. CERAM INT, **32**, 227 (2006). DOI: 10.1016/j.ceramint.2005.02.008
[5] S. Sasaki. J. STAM, **6**, 181 (2005). DOI: 10.1016/j.stam.2004.11.010
[6] L.P. Frank. J. APSUSC, **258**, 2639 (2012). DOI: 10.1016/j.apsusc.2011.10.110
[7] A. Mishra. J. APSUSC, **3** (4), 373 (2015). DOI: 10.1016/j.jascer.2015.08.004
[8] F. Zhang, Zh. Fu, J. Zhang, H. Wang, W. Wang, Yu. Wang, J. Shi. J. CERAMINT, **36**, 1491 (2010). DOI: 10.1016/J.CERAMINT.2010.02.013
[9] Y. Huang. J. CEJ, **220**, 143 (2013). DOI: 10.1016/J.CEJ.2013.01.059
[10] I. Solodkyi. J.CERAMINT, **45**, 168 (2019). DOI: 0.1016/J.CERAMINT.2018.09.148
[11] P.G. Karandikar. Mater. Sci., **29**, 163 (2009). DOI: 10.1002/9780470456286.CH16
[12] C. Wang. J. CERAMINT, **40** (6), 7915 (2014). DOI: 10.1016/J.CERAMINT.2013.12.139
[13] D. Zhou, S. Seraphin, J. C. Withers. Chem. Phys. Lett., **234** (1–3), 233 (1995). DOI: 10.1016/0009-2614(95)00039-7
[14] T.S. Orlova, V.V. Popova, J.Q. Cancap, D.H. Maldonado. J. JEURCERAMSOC, **31**, 1317 (2011). DOI: 10.1016/J.JEURCERAMSOC.2010.06.015
[15] Q. Wang. J. PARTIC, **7**, 199 (2009). DOI: 10.1016/j.partic.2009.01.011

[16] J. Li, Sh. Yu, Min Ge, X. Wei, Y. Qian. J. CERAMINT, **41**, 7853 (2015). DOI: 10.1016/J.CERAMINT.2015.02.122
[17] A. Gómez-Martín. J. CERAMINT, **42**, 16220 (2016). DOI: 10.1016/J.CERAMINT.2016.07.151
[18] M. Yu. J. CERAMINT, **46**, 5536 (2020). DOI: 10.1016/j.ceramint.2019.11.104
[19] E.O. Ademola, F.O. Bamigboye. *Proceedings of the iSTEAMS Multidisciplinary Cross Border Conference University of Professional Studies* (Accra Ghana, 2016)
[20] C.A. Eheverria, Farshid Pahlevani, S. Lim, V. Sahajwalla. J. JCLEPRO, **312**, 127808 (2021). DOI: 10.1016/j.jclepro.2021.127808
[21] A.Ya. Pak, P.S.Grinchuk, A.A. Gumovskaya, Yu.Z. Vassilyeva. J. CERAMINT, **48** (3), 3818 (2022). DOI: 10.1016/j.ceramint.2021.10.165
[22] A.Y. Pak. J. IJRMHM, **93**, 105343 (2020). DOI: 10.1016/j.ijrmhm.2020.105343
[23] R.S. Martynov, A.Ya. Pak, O.G. Volokitin, G.Ya. Mamontov. *Ustroystvo dlya polycheniya poroshka na osnove karbida bora.* Pat. № 210733 RF, MPK C01B 32/991 (2017.01) B22F 9/14 (2006.01) SPK C01B 32/991 (2022.02) B22F 9/14 (2022.02). № 2022102107: zayvl. 28.02.2022 g., opubl. 28.04.2022. (in Russian).
[24] K.V. Slyusarskiy, K.B. Larionov, V.I. Osipov, S.A. Yankovsky, V.E. Gubin, A.A. Gromov. J. FUEL, **191**, 383 (2017). DOI: 10.1016/J.FUEL.2016.11.087
[25] L. Xiaogang, Y. Zhou, D. Liu, B. Yang. NRL, **5**, 252 (2010). DOI: 10.1007/s11671-009-9474-8
[26] D. Zhou, S. Seraphin, J.C. Withers. CHEMICALPL, **234**, 233 (1995). DOI: 10.1016/0009-2614(95)00039-7
[27] Y. Saito, T. Matsumoto, K. Nishikubo. JCR, **172**, 163 (1997). DOI: 10.1016/S0022-0248(96)00709-9
[28] Yu.L. Krutskiy, G.G. Galevskiy, A.A. Kornilov. Poroshkovaya metallurgiya, **2**, 47 (1983) (in Russian).
[29] D. Liang, J.Liu, H. Li. J. Therm. Anal. Calorim., **128**, 1771 (2017). DOI: 10.1007/s10973-016-5989-2
[30] A. Jain, S. Anthonysamy. J. Therm. Anal. Calorim., **122**, 645 (2015). DOI: 10.1007/s10973-015-4818-3